Vol 14 No 10, October 2005
1009-1963/2005/14(10)/2061-07

Chinese Physics

© 2005 Chin. Phys. Soc.
and IOP Publishing Ltd

Study of sawtooth oscillations on the HT-7 tokamak using 2D tomography of soft x-ray signal*

Ma Tian-Peng(马天鹏)[a)†], Hu Li-Qun(胡立群)[a)], Wan Bao-Nian(万宝年)[a)], Ruan Huai-Lin(阮怀林)[b)], Gao Xiang(高 翔)[a)], Zhen Xiang-Jun(甄香君)[a)], Zhou Li-Wu(周立武)[a)], Sun You-Wen(孙有文)[a)], Chen Zhong-Yong(陈忠勇)[a)], Lin Shi-Yao(林士耀)[a)], and Kong Wei(孔 伟)[a)]

[a)] *Institute of Plasma Physics, Chinese Academy of Sciences, Hefei* 230031, *China*

[b)] *Institute of Electronic Engineering, Hefei* 230037, *China*

(Received 24 March 2005; revised manuscript received 25 June 2005)

It is the first time so far as we know that two arrays of multi-channel soft x-ray detectors are used to generate two-dimensional (2D) images of sawtooth oscillation on the HT-7 tokamak using the Fourier–Bessel harmonic reconstruction method, and using the singular value decomposition to analyse the data from soft x-ray cameras. By these two arrays, 2D image reconstruction of soft x-ray emissivity can be obtained without assumption of plasma rigid rotation. Tomographic reconstruction of the m=1 mode structure is obtained during the precursor oscillation of the sawtooth crash. The crescent-shaped mode structure appearing on the contour map of the soft x-ray emissivity is consistent with the quasi-interchange mode. The characteristics of the m=1/n=1 mode structure observed in the soft x-ray tomography are as follows: the magnetic surface is made up of the crescent-shaped "hot core" and the circular "cold bubble". The structure of the magnetic surface rotates in the direction of the electron diamagnetic drift and the rotation frequency is the oscillation frequency of soft x-ray signals.

Keywords: soft x-ray tomography, sawtooth oscillation, singular value decomposition (SVD)
PACC: 5270, 5270L

1. Introduction

The sawtooth oscillation, the most typical form of magnetohydrodynamic (MHD) activity, is a periodic collapse of the pressure or internal disruption in the plasma core. This regular periodic re-organization phenomenon of the core plasma surrounding the magnetic axis was first observed by von Goeler *et al* on the soft x-ray signals along a chord through the central region of the plasma in the ST tokamak.[1] Since then it has been observed on many diagnostics in all tokamaks, under different operation conditions corresponding to a broad range of plasma parameters. Experimental results in many tokamaks have convincingly shown that the sawtooth instability plays a crucial role in the formation of the temperature, density and current profiles in the centre of tokamak plasmas. Thus, sawtooth oscillation is a universal character in tokamak plasmas and is naturally supposed to affect significantly the fusion burning plasmas.[2] It has been attracting much interest, and considerable experimental and theoretical effort has been carried out to explain the mechanism.[3] Kadomtsev's full reconnection model is a standard two-dimensional (2D) model,[4] in which the hot core is a circle and the island is a crescent, the sawtooth crash based on the magnetic reconnection are induced by the shift of the hot core onto the q=1 surface due to the m=1/n=1 internal kink instability, where m and n are the poloidal and toroidal mode numbers, respectively. The model predicts that the hot plasma inside the q=1 surface is mixed with the cooler plasma outside in the course of successive reconnections of the helical magnetic flux inside and outside the q=1 surface. When the reconnection is completed, the plasmas are completely mixed. However, for large tokamaks such as JET, the predictions of Kadomtsev's model have many deviations from

*Project supported by the National Natural Science Foundation of China (Grant Nos 10375070 and 10305012).
†E-mail: tpma@ipp.ac.cn

some of the observed phenomena,[5,6] such as much shorter time to the sawtooth collapse and no precursor oscillations preceding the collapse of the compound sawtooth, etc. To solve these disagreements, Wesson's quasi-interchange mode was proposed,[7] in which the hot core is replaced by a cold bubble and the fast sawtooth crash is attributed to the kink flow drawing the cold bubble into the central region. The model predicts that the cold bubble enters the core plasma region and is surround by a closed surface. However, no comprehensive model has yet been developed to explain the experimental observations though much knowledge has been accumulated.

The sawtooth collapse is often in phase with the fall of the superimposed m=1 oscillation, but other cases show that sawtooth collapse is independent of the phase of the m=1 oscillation.[8–11] Therefore, it is very important that the amplitude and phase relationships between the superimposed m=1 oscillations and the m=0 sawtooth oscillations are studied in order to better characterize the relationship between the sawtooth collapse and the observed m=1 activity. One of the ways to confirm the theory of the sawtooth disruption is to compare the soft x-ray images obtained by the experiment with those predicted by the theory. This indirect method named cartography has been proposed to obtain the m=1 mode structure.[12]

In the HT-7 tokamak device, the sawtooth activity and other observed phenomena related to the plasma instability have been investigated experimentally using magnetic pick-up probes and other diagnostics. In this paper, in order to study the relationship between the sawtooth collapse and the observed m=1 activity, and to study in detail the characteristics of the sawtooth oscillations, tomography of the soft x-ray signal using multi-channel soft x-ray diode arrays is used to investigate sawtooth oscillations and m=1 mode. After a brief description of the soft x-ray system of the HT-7 tokamak in Section 2, the experimental results are presented in Section 3, and discussion is given in Section 4.

2. Experimental apparatus

HT-7 tokamak has major and minor radii of R_0=122cm and a=27cm, respectively. The soft x-ray diagnostic system, shown in Fig.1, consists of two imaging cameras with slot-apertures, which horizontally and vertically view a given toroidal cross-section of the plasma from different poloidal chords, each camera containing 37 Au–Si surface-barrier diode detectors.[13] All detectors are mounted on the arc-shaped stainless-steel pedestals with R=55cm in horizontal array and R=60cm in vertical array. Their spatial resolution, the radial distance between neighbouring viewing chords of the detectors, is 1.5cm. They view the plasma from –27cm to 27cm along given chords through thin slot-apertures with an area of 5mm×20mm in the vertical array and of 4mm×25mm in the horizontal array. This allows the use of a tomographic reconstruction method to obtain the local spatial distribution of the soft x-ray emission as a function of time without assuming rigid plasma rotation. The device operates normally at the following parameters:[14,15] plasma current I_p=100–250kA with a duration of 3–5s, central chord-averaged electron density $N_e(0)=(0.8\text{–}5.0)\times10^{13}\text{cm}^{-3}$,central electron and ion temperatures $T_e(0)$=0.5–1.0keV and $T_i(0)$=0.5keV, energy confinement time τ_E=15ms and effective charge Z_{eff}=2–3, and its major research fields focus on exploration of advanced steady-state operation, high-performance plasma discharge and plasma fuelling study including studies of lower hybrid current drive and lower hybrid wave (LHW) heating, and ion cyclotron range of frequency heating. The coordinate system which is used to designate the position and the view of each detector is shown in Fig.2. The origin of the coordinate system is placed at the centre of the vacuum vessel. The chords are denoted by $L(p,\phi)$. From the line-integrated measurements, the plasma image can be derived. This can provide much information on the plasma structure and the evolution of image with time, which is useful for studying the sawtooth oscillations and the MHD instabilities.The spatial profile of the soft x-ray emissivity is reconstructed by computer tomography based on the Fourier-Bessel expansion technique,[16] which is suitable for the circular plasma cross section in HT-7 tokamak.

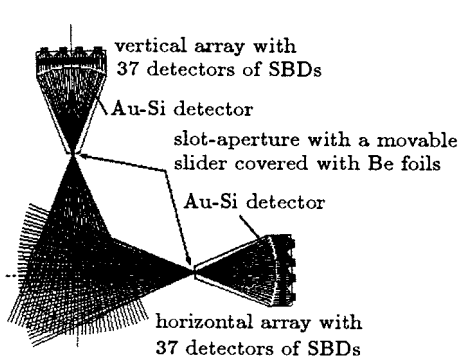


Fig.1. The soft x-ray imaging system on the HT-7 tokamak.

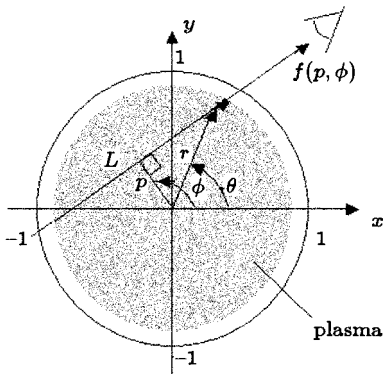


Fig.2. Coordinate system, where p is the chord impact parameter relative to the centre of the reconstruction, ϕ is the polar angle, and $f(p, \phi)$ is the chord brightness.

3. Experimental results

We have observed the sawtooth crash with the precursor oscillation on the intensity signal of the soft x-ray in the LHW and ion Bernstein wave (IBW) synergetic discharges with following plasma parameters: plasma currents $I_{\rm p}$ ≈127kA, central chord-averaged electron density $N_{\rm e}(0)$≈$1.36\times10^{13}{\rm cm}^{-3}$, a toroidal magnetic field at the plasma centre of $B_{\rm t}(0)$ ≈1.83T, $P_{\rm LHW}$ ≈141.5kW and $P_{\rm IBW}$ ≈151.5kW. Sawtooth oscillations of the soft x-ray signals near the centre for shot 54929 are shown in Fig.3 from 684.5ms to 692ms.

Using the singular value decomposition (SVD)

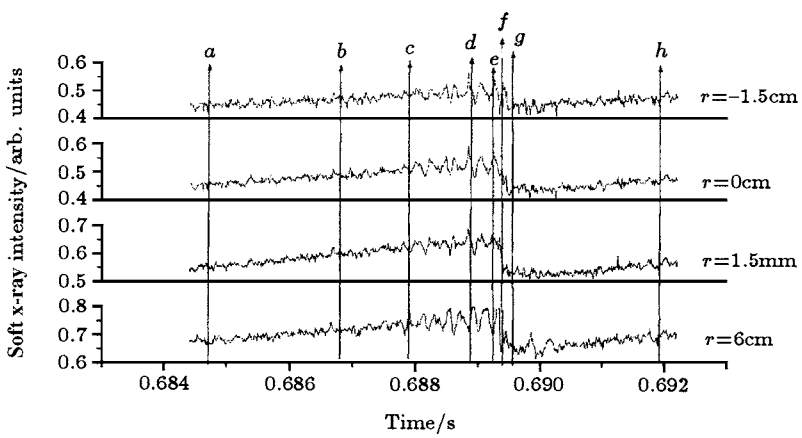


Fig.3. The discharge of the sawtooth waveforms of the shot 54929.

analysis,[17−22] we have obtained the temporal and the spatial structure of the sawtooth and the m=1/n=1 mode. Figure 4 shows the results of the SVD analysis. The first temporal eigenvector gives the evolution of the equilibrium emission, and its spatial eigenvector reflects the spatial distribution of soft x-ray emission. The sawtooth activity appears in the second component whose spatial eigenvector gives its reversal radius $r_{\rm s}$ ≈11.25cm, as shown in Fig.4(b). It is clear that the (1,1) mode perturbation is described by the third eigenvector. The temporal eigenvector reflects the m=1/n=1 mode repetition time about 0.217ms, as shown in Fig.4(a), while the spatial eigenvectors point to the characteristic radius r_1 ≈4.50cm, as shown in Fig.4(b). The spectrum in singular values from 1 to 37 is shown in Fig.4(c). The first three eigenvalues, whose quality of filtering is $\Delta_3 \approx 0.9896$, which reveals approximately three significant components containing almost all of the signal energy. The sawtooth component gives about 4.47% and the (1,1) mode component gives about 2.09% contribution to the raw signal. Therefore, in order to improve the signal-to-noise ratio by omitting the terms of small singular values, we choose the first three terms as the spatial-temporal signals in this paper. The contribution of the other terms to the total signal is small and noisy.

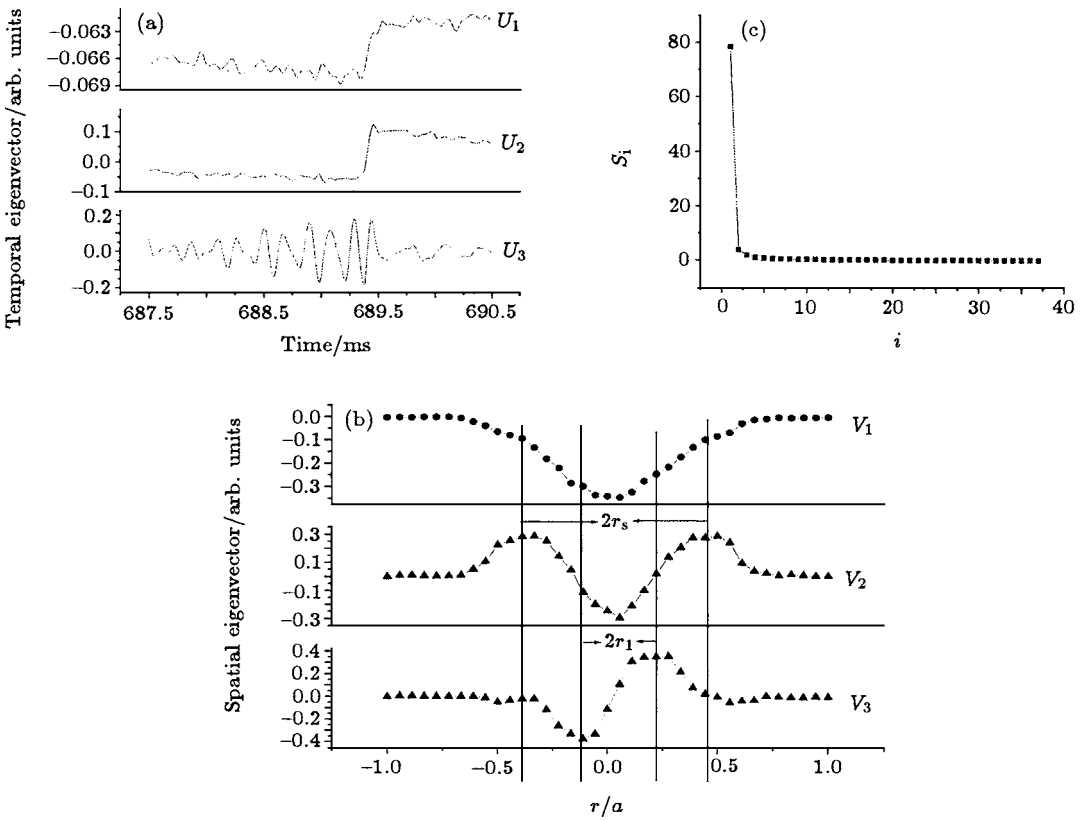


Fig.4. The results of the SVD analysis. (a) The first three temporal eigenvectors of the discharge #54929. The first temporal eigenvector U_1 gives the evolution of the equilibrium emission. The second temporal eigenvector U_2 gives the evolution of sawtooth activity.The temporal eigenvector U_3 corresponds to the (1,1) mode. (b) The first three spatial eigenvectors of the discharge #54929. The first spatial eigenvector V_1 reflects the spatial distribution of soft x-ray emission. The second eigenvector V_2 shows the spatial distribution of sawtooth activity. The spatial eigenvector V_3 corresponds to the spatial structure of the (1,1) mode. (c) Spectrum of the singular values from 1 to 37.

The main features of the crash in one sawtooth period seen on the contour plot of the emissivity map are illustrated in Fig.5, which are obtained by tomographic reconstruction of soft x-ray. Initially, the hot core moves outward along minor radius. The shape of the hot core changes from a circle to a crescent, a cold bubble appears in the opposite direction and grows gradually (from (c)–(f)). Here the region with low soft x-ray emissivity is defined cold, and the region with high emissivity is defined hot. The shape of the cold bubble becomes a circle when the cold bubble moves from the q=1 surface to the centre. Then, with the width of the cold bubble becoming wider and wider, the shape of the hot core becomes narrower and narrower (from (d)–(f)) during the ramp phase of the sawtooth oscillations. Before the crash, the cold bubble becomes largest and the crescent hot core moves to the $q = 1$ magnetic surface and its shape becomes narrowest, and at this moment, the crash of the sawtooth takes place. After the crash, the cold bubble is surrounded by a closed surface (Fig.5(g)). Finally, with the increase of the temperature, the cold bubble becomes a new hot core in the next period (Fig.5(h)), and the soft x-ray emissivity profile returns to the initial state and enters the next period.

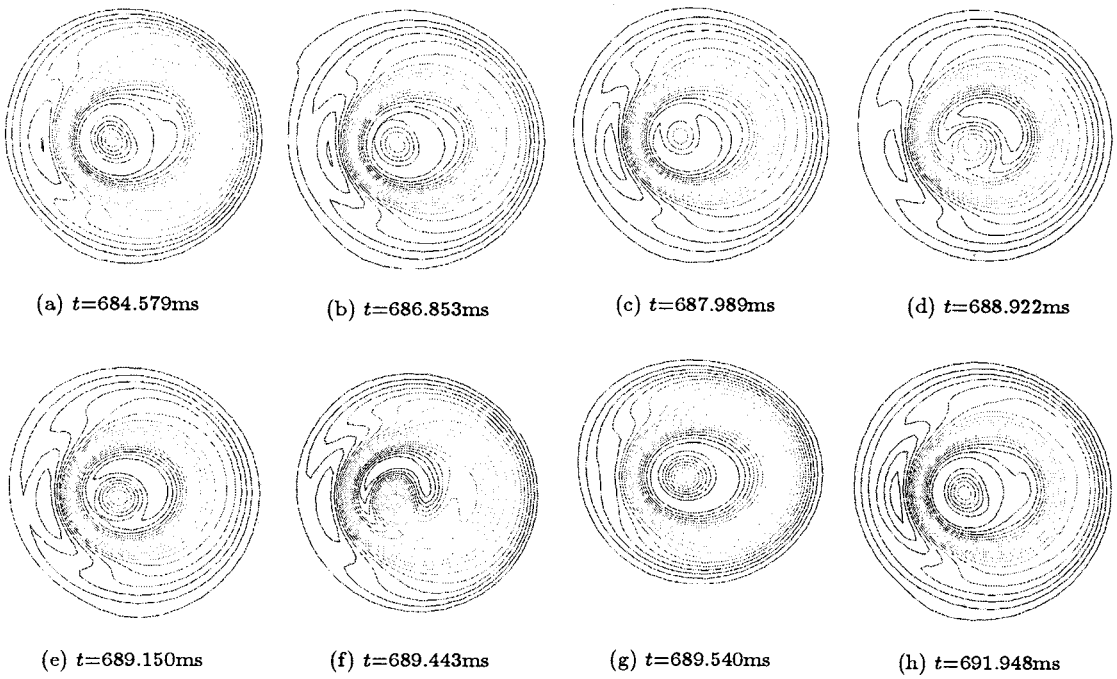


Fig.5. Contour plot of the reconstructed x-ray image during a sawtooth period.

In order to study the relationship between precursor oscillation on the sawtooth and the observed m=1 activity on soft x-ray intensity signals, more details on the precursor oscillation of the sawtooth crash has also been studied by the same tomography way, as shown in Figs.6 and 7. The soft x-ray signals and the time evolution of the tomographic image in one period of the $m = 1$ oscillations (from (a) to (h)) are shown in Fig.7. From the contour plot of the emissivity map, it is very clear that the hot core does not in the central region of the plasma, but moves outward to the vicinity of the q=1 surface. The shape of the hot core becomes crescent, and a circular cold bubble appears in the opposite direction. Therefore, the magnetic surface is made up of the crescent-shaped "hot core" and the circular "cold bubble". The structure of the magnetic surface rotates in the direction of the electron diamagnetic drift, and the rotation frequency is the oscillation frequency of soft x-ray signals. When the amplitude of the $m = 1$ oscillation increases, the shape of the hot core becomes narrower. After the crash of the sawtooth, the shape of the hot core changes from a crescent to a closed surface (Fig.5(g)).

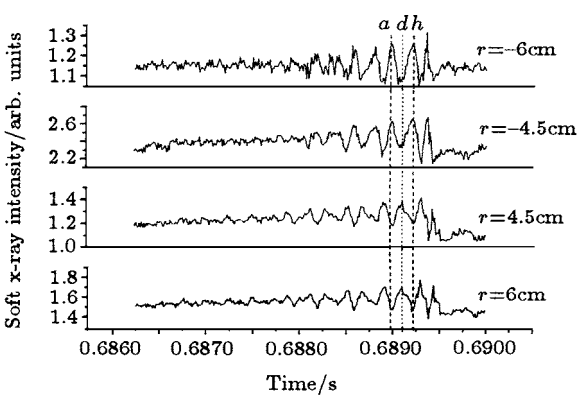


Fig.6. The m=1 oscillations near the centre soft x-ray signals for the shot 54929.

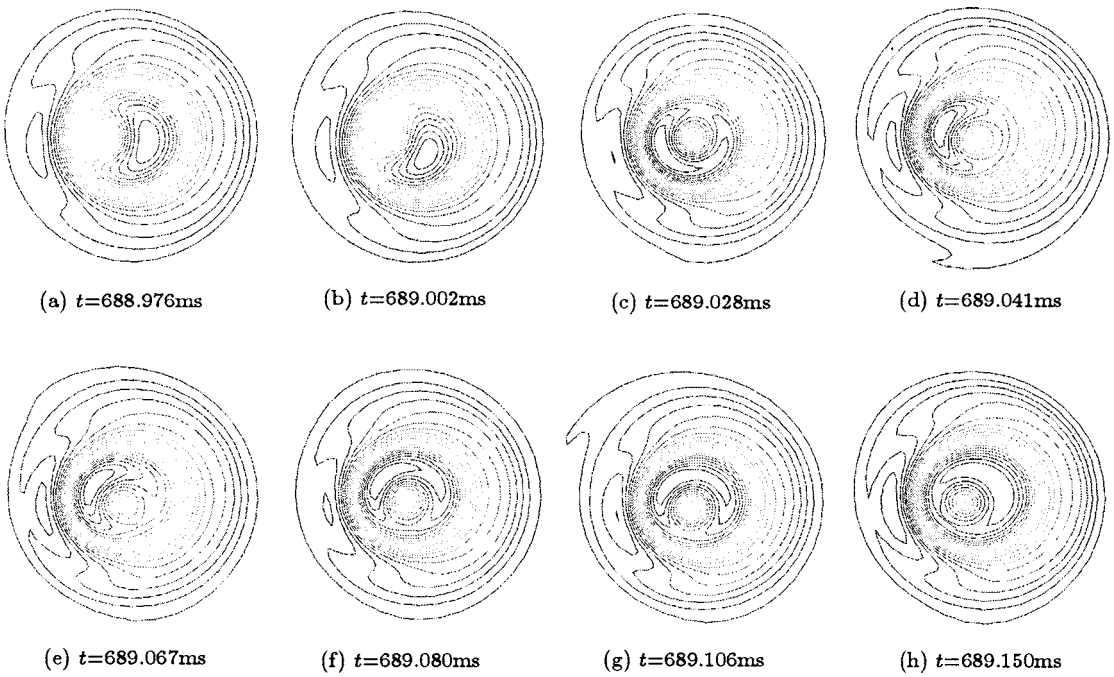


Fig.7. The contour plot of the emissivity map in one period of the m=1 oscillation.

4. Discussion

The analysis of sawtooth activity has been given in last section. But it is a pity that we did not know some of the detailed parameter profiles, such as $q(r)$. Furthermore, it is difficult to completely explain the sawtooth behaviour even today. Therefore, we can give only a qualitative analysis of the sawtooth oscillation.

As is known, the hot core includes the largest densities, and its temperature increases more rapidly than other parts. So, the pressure becomes higher in the core part than other due to the LHW and IBW synergetic heating, which may drive the hot core to move outward. Figure 8 shows the spatial profiles of the soft x-ray emission intensity during one period of the sawtooth oscillation. Variations of the soft x-ray emission intensity roughly reflect the changes of the pressure. The spatial profile of soft x-ray emission at time 689.150ms is more peaked than at time 684.579ms, and the gradient at the sawtooth reversal surface at time 689.150ms is larger than at time 684.579ms. It is suggested that the pressure gradient at the sawtooth reversal surface at time 689.150ms is larger than that at time 684.579ms. The peaked soft x-ray profile is broadened after the sawtooth crash at time 689.540ms. Hence, it is possible that the pressure-driven instability can be induced by the shift of the hot core.

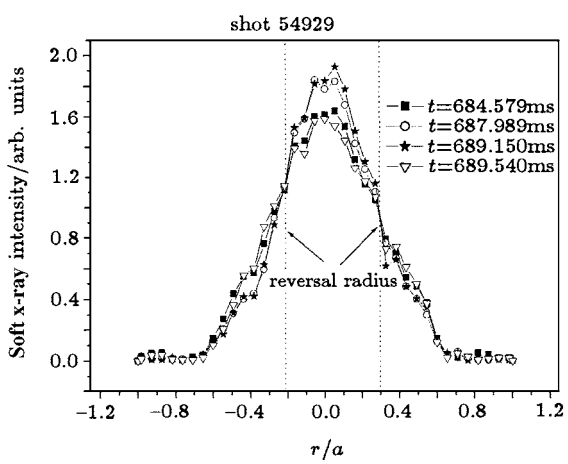


Fig.8. The spatial profile of the soft x-ray signals before and after the sawtooth crash.

We have assumed implicitly that the high soft x-ray emission region has a high electron temperature. However, the local soft x-ray emissivity is generally a function of the electron temperature and the electron impurity densities. It is quite difficult to determine accurately how much each factor contributes to the local soft x-ray emissivity. This has been an unresolved question regarding soft x-ray images in previous studies also. For example, in a very high temperature plasma heated by powerful neutral beam injection in the TFTR tokamak, high-Z metallic impurity emissions dominated in soft x-ray emissions and soft x-ray images did not reflect the electron temperature contours.[23] That is, the core soft x-ray emissivity decreased by 75% during the crash, while the electron temperature and density decreased by only 10%. This

result is ascribed to a strong accumulation of metallic impurities in the plasma core due to the high-Z ion pinch effect. Furthermore, one of the main reasons is that the strong accumulation of metallic impurities, such as ferrum, nickel etc, which could not be excluded, would induce the core plasma cold after the crashes (Fig.5(g)).

Finally, as described in Ref.[24], where the authors pointed out that artifacts can appear in soft x-ray images based on the Fourier–Bessel expansion technique when the angular mode numbers used for computer tomography imaging are not sufficient. Especially, an off-centred circular hot core pushed on the inversion radius in the case of Kadomtsev type of crash looks like a crescent shape if numbers used for the angular expansion are restricted to m=0 and 1. Angular mode numbers up to m=3 are sufficient to distinguish the crescent shape from the circular one. Therefore, in all soft x-ray images in this paper, mode numbers up to m=2 and l=7 have been used for the angular and radial expansions, respectively, which is determined with the help of the Akaike information criterion.[25]

Perhaps, these results might correspond to the two-step model for the sawtooth crash. That is, magnetic reconnection proceeds gradually in the first phase in the manner suggested by Kadomtsev. In the second phase, the fast sawtooth crash is attributed to the kink flow drawing the cold bubble into the central region, as suggested by Wesson. But, it is quite clear that the Wesson's model process is a domain effect in the sawtooth process, i.e. the convective flow of colder plasma into the centre core causes the sawtooth crash.

In conclusion, using 74 soft x-ray detectors at one toroidal location, we have obtained tomographic reconstructions of the soft x-ray emissivity without assuming any rigid rotation of the plasma, and applied pre-processing and post-processing SVD technique, which is a powerful tool well suited to the study of spatial-temporal signals, and to the tomography reconstructed image in order to obtain clearer profile. During the ramp phase of the sawtooth, the hot core deviates from the centre of plasma to the vicinity of the q=1 surface, and the shape changes from a circle to a crescent gradually. Meanwhile, a circular cold bubble appears in the opposite direction and grows gradually. Before the crash, the cold bubble becomes largest and the crescent hot core is moved to the q=1 magnetic surface and its shape becomes narrowest. After the crash, the shape of the hot core changes from a crescent to a closed surface and with the increase of the temperature in the centre plasma, the cold bubble becomes a new hot core in the next period. The crescent-shaped mode structure appearing on the contour map of the soft x-ray emissivity is consistent with the Wesson's quasi-interchange mode. In one period of the $m = 1$ oscillations, the magnetic surface structure is made up of the crescent-shaped "hot core" and the circular "cold bubble". The structure of the magnetic surface rotates in the direction of the electron diamagnetic drift, and the rotation frequency is the oscillation frequency of the m=1, n=1 mode.

Acknowledgment

The authors would like to thank Professor Yi Liu (South-Western Institute of Physics, Chengdu, China) for valuable discussions.

References

[1] von Goeler S *et al* 1974 *Phys. Rev. Lett.* **33** 1201
[2] porcelli F *et al* 1996 *Plasma Phys. Control. Fusion* **38** 2163
[3] Hastie R J 1998 *Astrophys. Space Sci.* **256** 177
[4] Kadomtsev B B 1975 *Sov. J. Plasma Phys.* **1** 389
[5] Campbell D J *et al* 1987 *Proc. 12th IAEA Conf. on Plasma Phys. and Control. Nucl. Fusion Res. Nice*, France, IAEA, Vienna **2** 433
[6] Campbell D J *et al* 1986 *Nucl. Fusion* **26** 1085
[7] Wesson J A 1986 *Plasma Phys. Control. Fusion* **28** 243
[8] EQUIPE TFR 1977 in *Plasma Physics and Controlled Nuclear Fusion Research* 1976 (Proc, 6th Int. Conf. Berchtesgaden, 1976) IAEA, Vienna **1** 279
[9] Dubois M *et al* 1979 in *Plasma Physics and Controlled Nuclear Fusion Research* 1978 (Proc. 7th Int. Conf. Innsbruck) IAEA, Vienna **1** 615
[10] EQUIPE TFR 1983 in *Plasma Physics and Controlled Nuclear Fusion Research* 1982 (Proc, 9th Int. Conf. Baltimore, 1982) IAEA, Vienna **3** 383
[11] Dubois M A *et al* 1983 *Nucl. Fusion* **23** 147
[12] Dubois M A *et al* 1980 *Nucl. Fusion* **20** 1355
[13] Hu L Q *et al* 2000 *Plasma Sci. Technol* **2** 515
[14] Shi Y J *et al* 2005 *Chin. Phys.* **14** 1193
[15] Hu L Q *et al* 2003 *Plasma Phys. Control. Fusion* **45** 349
[16] Nagayama Y 1987 *J. Appl. Phys.* **62** 2702
[17] Nardine C 1992 *Plasma Phys. Control. Fusion* **34** 1447
[18] Kim J S *et al* 1999 *Plasma Phys. Control. Fusion* **41** 1399
[19] Marrelli L *et al* 2001 *Rev. Sci. Instrum.* **72** 499
[20] Dudok de Wit T *et al* 1994 *Phys. Plasmas* **1** 3288
[21] Dudok de Wit T 1995 *Plasma Phys. Control. Fusion* **37** 117
[22] Anton M *et al* 1996 *Plasma Phys. Control. Fusion* **38** 1849
[23] Nagayama Y *et al* 1991 *Phys. Rev. Lett.* **67** 3527
[24] Janicki C *et al* 1989 *Phys. Rev. Lett.* **62** 3038
[25] Akaike H 1974 *IEEE Trans. Autom. Control.* **AC-19** 78